Heliyon 9 (2023) e16056

Contents lists available at ScienceDirect

Heliyon

journal homepage: www.cell.com/heliyon

Research article

Spatio-temporal multidisciplinary analysis of socio-environmental conditions to explore the COVID-19 early evolution in urban sites in South America

Gilma C. Mantilla Caicedo [a], Matilde Rusticucci [b], Solange Suli [b], Verónica Dankiewicz [b], Salvador Ayala [c], Alexandra Caiman Peñarete [d], Martín Díaz [e], Silvia Fontán [e], Francisco Chesini [f], Diana Jiménez-Buitrago [g], Luis R. Barreto Pedraza [h], Facundo Barrera [i,j,*]

[a] *Global Consortium on Climate and Health Education, Columbia University, New York, United States*
[b] *Universidad de Buenos Aires, Departamento de Ciencias de la Atmósfera y los Océanos, CONICET, Argentina*
[c] *Universidad de Chile, Programa de Doctorado en Salud Pública, Instituto de Salud Pública de Chile, Chile*
[d] *Subred Integrada de Servicios Hospitalarios Centro Oriente ESE, Red Hospitalaria Bogotá Distrito Capital, Colombia*
[e] *Universidad Nacional de La Matanza, Departamento de Ciencias de la Salud, Argentina*
[f] *Ministerio de Salud de Argentina, Argentina*
[g] *Ministerio de Salud y Protección Social, Mesa de Variabilidad y Cambio Climático de la CONASA, Colombia*
[h] *Instituto de Hidrología, Meteorología y Estudios Ambientales - IDEAM, Subdirección de Meteorología, Mesa de Variabilidad y Cambio Climático de la CONASA, Miembro del grupo QuASAR UPN, Colombia*
[i] *Centro Austral de Investigaciones Científicas (CADIC), Consejo Nacional de Investigaciones Científicas y Técnicas (CONICET), Ushuaia, Argentina*
[j] *Centro i~mar, Universidad de Los Lagos, Chile and Centre for Climate and Resilience Research (CR)2, Casilla 557, Puerto Montt Chile*

ARTICLE INFO

Keywords:
Climate variability
SARS-CoV-2
Pandemic
GINI
Parametric and non-parametric analysis

ABSTRACT

This study aimed to analyse how socio-environmental conditions affected the early evolution of COVID-19 in 14 urban sites in South America based on a spatio-temporal multidisciplinary approach. The daily incidence rate of new COVID-19 cases with symptoms as the dependent variable and meteorological-climatic data (mean, maximum, and minimum temperature, precipitation, and relative humidity) as the independent variables were analysed. The study period was from March to November of 2020. We inquired associations of these variables with COVID-19 data using Spearman's non-parametric correlation test, and a principal component analysis considering socio economic and demographic variables, new cases, and rates of COVID-19 new cases. Finally, an analysis using non-metric multidimensional scale ordering by the Bray-Curtis similarity matrix of meteorological data, socio economic and demographic variables, and COVID-19 was performed. Our findings revealed that the average, maximum, and minimum temperatures and relative humidity were significantly associated with rates of COVID-19 new cases in most of the sites, while precipitation was significantly associated only in four sites. Additionally, demographic variables such as the number of inhabitants, the percentage of the population aged 60 years and above, the masculinity index, and the GINI index showed a significant correlation with COVID-19 cases. Due to the rapid evolution of the COVID-19 pandemic, these findings provide strong evidence that biomedical, social, and physical sciences should join

* Corresponding author. Centro Austral de Investigaciones Científicas (CADIC), Consejo Nacional de Investigaciones Científicas y Técnicas (CONICET), Ushuaia, Argentina.
E-mail address: facundobarrera182@gmail.com (F. Barrera).

https://doi.org/10.1016/j.heliyon.2023.e16056
Received 1 December 2021; Received in revised form 24 April 2023; Accepted 3 May 2023
Available online 6 May 2023

forces in truly multidisciplinary research that is critically needed in the current state of our region.

1. Introduction

In the twenty-first century, we have been dealing with the coronavirus (COVID-19) pandemic caused by the SARS-CoV-2 virus [1–3]. Because of globalization and anthropogenic activities [4–6], natural alterations or changes in SARS-CoV-2 have created significant risks to human health over time [7–9]. By November 2020, more than 62 million confirmed cases of COVID-19 had been reported, with approximately 1.5 million human deaths [10]. Pan American Health Organization reported more than 26 million confirmed cases and accounted for half of the deaths worldwide in America [11].

The interaction between host and pathogen can be significantly affected by environmental conditions, either directly, such as by improving transmission rates of the pathogen, or indirectly, by affecting the susceptibility of the host to pathogenic attacks [12]. Climate conditions can influence the trajectory of the pandemic, and the seasonal progression of the disease will lead to different implications across the globe, varying by hemisphere, region, and climatic zone [13,14].

Different pathologies, especially respiratory system diseases, are significantly associated with certain unfavourable climatic conditions that predisposes people to develop those diseases [15–17]. In the case of COVID-19, climate conditions as top predictors of other coronavirus illnesses [18,19] as wind speed, humidity [20,21], average air temperature, and vapour pressure, which are measures of absolute humidity, are critical in the transmission of infectious diseases [22,23]. Previous studies have shown that survival is generally higher at low temperatures and low absolute humidity values in the case of coronavirus and influenza viruses [20,24]. For each country/region and specific climatic differences between regions, the effect of UV light on the survival of the virus on surfaces, or higher temperatures have a significant impact on the current spread of the SARS-CoV2 virus [25]. Other authors have reported that in similar viral diseases (such as pneumonia), mortality rates are highly correlated with weather changes [26]. There is also a high correlation between climate indicators and the spread of the COVID-19 pandemic in North America [27]. In the case of Latin América and the Caribbean region, Bolaño-Ortiz et al. (2020) [15] studied the relationship during two months in austral fall 2020 and concluded that average and minimum temperature and air quality were significantly associated with the spread of COVID-19 in ten

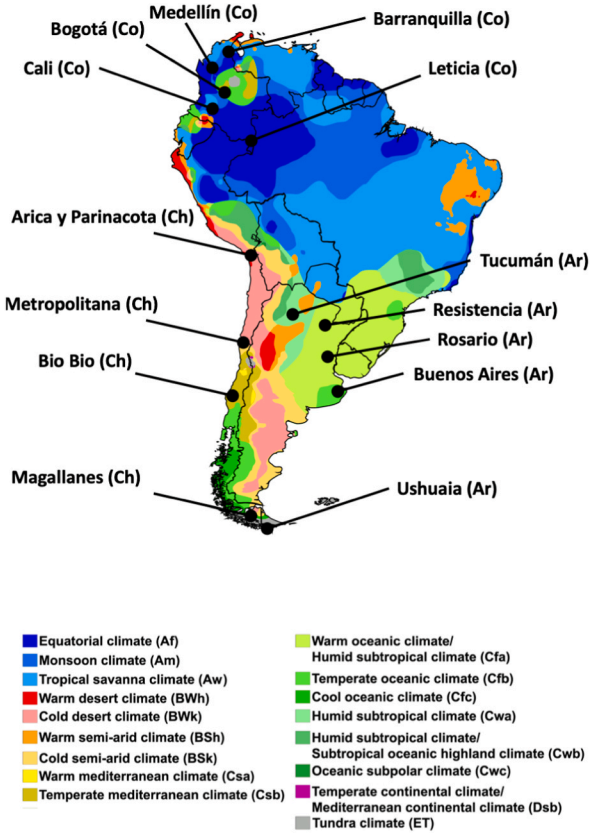

Fig. 1. Climatic characterization and sites of study in South America. Colour scale according the climate category. Adapted from Beck [4]. (For interpretation of the references to colour in this figure legend, the reader is referred to the Web version of this article.)

cities of the region. Humidity, wind speed, and rainfall also showed a significant relationship with morbimortality for various cities.

In addition to effects of climatic variables on respiratory diseases, it is well documented that socioeconomic and demographic conditions are another group of influencing factors. Studies conducted in different regions of the world (United Kingdom, Europe, China, North America) have shown effects of socio-economic conditions on the impact of the COVID-19 pandemic [28–30]. Variables that have demonstrated correlation to the spread of COVID 19 have been population density, employment rate, and poverty rate, among others [31]. Studies analysing the association between socioeconomic conditions and the pattern of the pandemic in the South American region are still lacking.

Some demographic aspects could have a significant influence in the high number of cases [32,33] and deaths during the pandemic worldwide [34,35]. In fact, South America may be one of the regions most affected by this public health crisis [36–39] because it has notorious resource limitations in their health systems. Therefore, this study aims to provide strong evidence that spatio-temporal multidisciplinary analysis of socio-environmental conditions can be used to demonstrate the early evolution of COVID-19 in urban sites in South America.

2. Materials and methods

2.1. Study areas in South America

The study considered 14 urban sites (Fig. 1) with heterogeneous population distribution and dissimilar climatic, geographical, socioeconomic and demographic conditions from Colombia (CO), Chile (CH), and Argentina (AR) (Table Supp 1). Five representative sites were chosen in Colombia, from north to south: Barranquilla, Medellín, Bogotá, Cali, and Leticia. In Chile, four sites were analysed: Arica y Parinacota, Centre Metropolitana, Biobío, and South Magallanes. In Argentina, five sites were analysed: Tucumán, Resistencia, Rosario, the Autonomous City of Buenos Aires (Buenos Aires), and the southernmost city of South America, Ushuaia.

2.2. Meteorological, Socioeconomic and demographic data set

We employed public data set of different state organism (Table 1). Data of COVID-19 cases from each urban site obtained from daily reports by the Ministry of Health (National Directorate of Epidemiology and Strategic Health Information of the Ministry of Health) of Argentina, the Ministry of Health of Chile, and the Ministry of Sciences and the database of the Integrated Social Protection Information System of the Ministry of Health and Social Protection of Colombia. The period considered was March 2020 to November 2020. Additionally, we used daily national meteorological data: maximum, mean, and minimum temperature (T_{max}, T_{mean} and T_{min}), precipitation (Pp), and relative humidity (Hr), obtained from National Meteorological Service (Argentina), Meteorological Directorate (Chile), and Institute of Hydrology, Meteorology, and Environmental Studies (Colombia), through the network of manual (AR) and automatic (CH and CO) weather stations placed across the cities of study. Annual socio-economic and demographic data were obtained from National Institute of Statistics and Census (Argentina), National Statistics Institute, Ministry of Social Development, National Socioeconomic Characterization Survey (Chile) and National Administrative Department for Statistics, National Population and

Table 1
Summary of data set access used to this study from March 2020 to November 2020. COVID-19 (New cases with symptoms (NCS) and rate of new cases with symptoms (rNCs) by day and per 100.000 inhab.). Meteorological data. Relative humidity (Hr. %). Precipitation (Pp. mm); and maximum. Mean and minimum temperature (T_{max}. T_{mean} and T_{min}. °C) to each site sampled.

Variables Group	Variable Order	Metadata access of each Country	link acces
COVID-Cases	• New cases with symptoms (NCS) • Rate of new cases with symptoms by day and per 100.000 inhab (rNCS) • 7 and 14-day moving averages (7rNCSma and 14rNCSma) • 7- and 14-day lags of the rNCS (7rNCSL and 14rNCSL)	Ministry of Health (AR) Ministry of Health (CH) Ministry of Health and Social Protection (CO)	https://www.datos.salud.gob.ar/dataset?groups=covid-19 https://www.minsal.cl/nuevo-coronavirus-2019-ncov/ https://www.ins.gov.co/Noticias/paginas/coronavirus.aspx
Socio-demographic Data Set	Population index • nº inhabitants (x 103 inhab) • Density (δ. inhab km-2) • Population over 60 years (%) Socio-economic index • Monetary Poverty (%) • Masculinity Index (%) • GINI	National Institute of Statistics and Census (AR) National Statistics Institute (CH) National Administrative Department for Statistics. National Population and Housing Census (CO)	https://www.indec.gob.ar/ https://www.ine.gob.cl/ https://www.dane.gov.co/
Meteorological Deata Ser	• Relative humidity (Hr. %) • Precipitation (Pp. mm) • Temperature mean (Tmean. °C) • Temperature maximum (Tmax. °C) • Temperature minimum(Tmin. °C)	National Meteorological Service (AR) Meteorological Directorate (CH) Institute of Hydrology. Meteorology. And Environmental Studies (CO)	https://www.smn.gob.ar/ https://www.meteochile.cl/PortalDMC-web/index.xhtml https://www.ideam.gov.co/

Housing Census (Colombia).

2.3. Statistical data analyses

Exploratory analysis was carried out to finalize the possible associations with the COVID-19 data new daily cases with symptoms (NCS) and rate of new daily cases with symptoms (rNCS) using Spearman's non-parametric correlation test. Subsequently, principal component analysis (PCA) was used to reduce the dimensionality [40] and establish an association between them [31]. This technique was used as it is a particularly useful multivariate statistical method in reducing a large group of variables to a smaller group of latent underlying factors that explain most of the observed variability. A second analysis was performed using non-metric multidimensional scaling ordination (nMDS) using the Bray-Curtis matrix of similarity cluster analyses to identify common socio-economic and environmental attributes among different sites, using vegan [41] and Nbclust [42] packages respectively, were performed in RStudio software Version 1.4.1717. (https://rstudio.com/). Since data on new cases with symptoms were available from the date of confirmation, we decided to use the rate of new cases with symptoms with a 7-day lag for a comparative study (Table Supp 2).

Subsequently, for each site, the daily incidence rNCS was analysed per 1 × 105 inhabitants (inhab.) by the date of symptom onset (Argentina and Colombia) and by date of confirmation (Chile). Seven- and 14-day moving averages (7rNCSma and 14rNCSma) were applied to smooth the dummy wave generated by data loading. In addition, the 7- and 14-day lags of the rNCS with a 7-days moving average (7rNCSL and 14rNCSL) were calculated considering the incubation period of the disease. Likewise, a description was made of the statistical distribution of variables studied, dependent rNCS, and independent (meteorological-climatic data). The coefficient of variation was calculated according to equation I (Eq. (1)) and was percentually expressed as:

$$CV_n = Std_n\ X_n * 100 \tag{1}$$

where Std is the standard deviation, and X is the mean of each sample (n) by site.

Finally, the statistical distribution of the data was analysed using the Shapiro-Wilk test [43,44], and it was observed that variables did not maintain a normal distribution. Therefore, Spearman's linear correlation [44] was used to study the relationship between rNCS and different climatic variables. From this, the 'rho = ρ' coefficient was obtained with confidence levels of 95% and 99%. All calculations were performed using RStudio software Version 1.4.1717. (https://rstudio.com/).

3. Results

3.1. Climatic variability characterization by site

In Argentina, most sites have a humid subtropical climate (Table 2, climate code: Cfa), which is characterised by relatively high temperatures and evenly distributed precipitation throughout the year, with the exception of Ushuaia, which has a Tundra Climate (Table 2, climate code: AT). This climate is characterised by sub-freezing mean annual temperatures, large annual temperature ranges, and moderately low precipitation [45]. The temperature drops between March and June and rises between June and October. Accumulated Pp is the highest in the north of the country, with maximum monthly values in Tucumán (approximately 240 mm) and Resistencia (approximately 200 mm) during 1981–2010, decreasing towards the west, centre, and south of the country where it is scarce. In the northern and central regions (Tucumán, Resistencia, Rosario, and Buenos Aires), the annual wave of monthly Pp is minimal in the winter (June to August). The opposite occurs in Patagonia, with a maximum around 55 mm in winter (as is the case of Ushuaia) (https://www.smn.gob.ar/clima/vigilancia). In general, Pp was higher in the northern and central regions than in southern

Table 2
Geographical position. Altitude. And climate codes [45] from study sites in South America. Cfa. temperate. no dry season. warm summer; ET. polar. tundra; Bwh. Arid. desert. hot; Csb. temperate. dry summer. warm summer; Aw. tropical. savannah; Af. tropical. Rainforest; Cfb. temperate. no dry season. warm summer.

Sites	Latitude	Longitude	Altitude (msal)	Climate Code
Tucuman (Ar)	26°49′26.9″ S	65°13.356′ W	431	Cfa
Resistencia (Ar)	27°27′38″ S	58°59.033′ W	50	Cfa
Rosario (Ar)	32°56′48.6″ S	60°38.359′ W	31	Cfa
Buenos Aires (Ar)	34°36′47.3″ S	58°22.634′ W	25	Cfa
Ushuaia (Ar)	54°48′39″ S	68°18.955′ W	200	ET
Arica y Parinacota (Ch)	18°28′30″S	70°18′52″ W	40	BWh
Metropolitana (Ch)	33°26′16″S	70°39′01″W	544	Csb
Biobío (Ch)	36°46′22″S	73°03′47″W	119	Csb
Magallanes (Ch)	53°09′45″S	70°55′21″W	214	ET
Barranquilla (Co)	10° 59′ 16″ N	74° 47′ 20″ W	18	Aw
Medellín (Co)	6° 13′ 1″ N	75° 34′ 1″ W	1495	Af
Bogotá (Co)	4° 35′56″ N	74°04′51″ W	2630	Cfb
Cali (Co)	3° 26′ 14″ N	76° 31′ 21″ W	1018	Af
Leticia (Co)	4° 12′ 29″ S	69° 56′ 36″ W	80	Af

Patagonia. The temperature followed the same pattern as Pp (Table 3, Fig. 1).

Colombia is one of the countries with the greatest rainfall diversity in the world (Fig. 1). Medellin, Cali, and Leticia have a tropical rainforest climate (Table 2, climate code: Af) with no dry season, and all months have a Pp of at least 60 mm. Regions with this climate are typically hot and wet throughout the year with both heavy and frequent rainfall. On the other hand, Barranquilla has a tropical savanna climate (Table 2, climate code: Aw) with a $T_{mean} > 18$ °C and Pp < 60 mm monthly average. This climate experiences either less rainfall than a tropical monsoon climate or more pronounced dry seasons. Bogotá is characterised by an equable climate with few extremes of temperature and ample precipitation in all months, which is a typical marine west coast climate (Table 2, climate code: Cfb) [45].

Historically, the sites Barranquilla, Medellín, Bogotá, and Cali presented a Pp behaviour characterised by a seasonal cycle of two periods of little rain (dry periods) and two rainy periods. This varied according to the latitude and its orographic conditions, which were observed in the duration of each season and in the value of Pp. The temporal distribution of Pp was characterised by a cycle of a dry period (May–October) and a rainy period (November–April). The rainiest city was Leticia, with an annual accumulated value of >3300 mm year-1, located to the south of the equator [46]. The site with the highest variability in T_{max}, T_{mean}, and T_{min} was found in Barranquilla (Table 3, Fig. 2a). Bogotá showed the lowest temperature value (Table 3, Fig. 2a).

The Hr was 55%–89% on average for all the test regions. In the north sampling area, Hr had two periods of high and low values equal to the Pp according to the ITCZ (Fig. 2b). In Bogotá, the Hr was 77%–83%, being higher in the months of April and November and lower in July and August. In Medellin, Hr was 63%–73% and higher at the time of the 2nd semester, but lower than that at other sites (Table 3. Fig. 2b). The Hr in Cali was <70% in dry periods and 75%–76% in rainy periods. In Leticia, Hr (84%–88%) was high during the 1st semester and relatively low in August and September. The proximity to the sea and the location on the banks of the Magdalena River mean that Barranquilla had a high Hr. However, this Hr was modified by drying winds that pushed it toward the interior of the region to produce abundant rains in the foothills of the Andes. In Barranquilla, the highest levels of Hr (about 84%) were registered in October, with the minimum levels in February and March (77%) (Table 3, Fig. 2b).

The north of Chile is arid because of the Atacama Desert, while that of southern Chile is temperate, ranging from the Mediterranean to the marine west coast [47] (Fig. 1). In Arica y Parinacota, tropical and subtropical desert climates (Table 2, climate code: BWh) were dominant in all months. This was because the subtropical anticyclone, or subtropical high, had winds blow parallel to the coast so that moisture-laden maritime air could penetrate over land only infrequently and inhibit precipitation. Metropolitana and Biobío sites had a typical Mediterranean climate (Table 2, climate code: Csb) with very dry and warm summers. Summers had one-third the Pp of the wettest winter month, and with Pp < 30 mm in a summer month (Fig. 2a–b). The Magallanes site was similar to Ushuaia (Table 2,

Table 3
Mean ± standard deviation and coefficient variation [cv] of COVID-19 new daily cases with symptoms (NCS) and rate of new cases with symptoms (rNCS) per 100.000 inhab. And meteorological data: relative humidity (Hr. %), precipitation (Pp. mm) and maximum, mean and minimum temperature (Tmax, Tmean and Tmin. °C) of each site sampled.

Sites	COVID-19 data		Environmental data				
	NCS	rNCS	Hr [%]	PP [mm]	T_{max} [°C]	T_{mean} [°C]	T_{min} [°C]
Tucumán (AR)	30.55 ± 43.92 [143.8]	5.57 ± 8.00 [143.8]	62.07 ± 15.27 [24.6]	0.97 ± 5.31 [544.86]	26.31 ± 6.18 [23.48]	19.47 ± 5.55 [28.49]	12.63 ± 5.94 [47.02]
Resistencia (AR)	20.00 ± 12.59 [62.94]	5.12 ± 3.22 [62.94]	64.07 ± 13.89 [21.68]	1.68 ± 6.86 [408.09]	28.71 ± 6.84 [23.83]	21.25 ± 6.18 [29.09]	13.8 ± 6.38 [46.23]
Rosario (AR)	159.74 ± 221.11 [138.42]	13.33 ± 18.45 [138.42]	63.98 ± 14.8 [23.13]	1.68 ± 8.37 [496.64]	23.56 ± 6.18 [26.23]	16.61 ± 5.8 [34.93]	9.65 ± 6.39 [66.23]
Buenos Aires (AR)	344.93 ± 264.7 [76.74]	11.93 ± 9.16 [76.74]	68.36 ± 12.77 [18.68]	2.38 ± 8.45 [355.01]	21.28 ± 5.3 [24.89]	16.73 ± 5.06 [30.24]	12.19 ± 5.25 [43.11]
Ushuaia (AR)	14.16 ± 23.5 [165.97]	24.87 ± 41.27 [165.97]	72.98 ± 10.76 [14.74]	1.04 ± 2.17 [208.28]	7.8 ± 8.06 [103.31]	5.54 ± 3.91 [70.59]	2.88 ± 3.29 [114.24]
Arica y Parinacota (CH)	27.81 ± 26.47 [95.17]	12.3 ± 11.71 [95.17]	70.51 ± 3.93 [5.58]	0.0 ± 0.0 [-]	20.87 ± 2.79 [13.39]	18.25 ± 2.46 [13.5]	16.59 ± 2.36 [14.2]
Metropolitana (CH)	840.88 ± 1145.91 [136.27]	11.82 ± 16.11 [136.27]	67.87 ± 13.55 [19.96]	0.69 ± 4.03 [585.55]	22.29 ± 6.18 [27.74]	13.07 ± 4.44 [33.97]	6.76 ± 3.52 [51.99]
Bíobío (CH)	105.04 ± 72.75 [69.26]	6.75 ± 4.67 [69.26]	81.71 ± 10.31 [12.62]	2.88 ± 7.4 [256.54]	16.65 ± 3.48 [20.88]	11.59 ± 2.78 [24.03]	7.76 ± 3.39 [43.66]
Magallanes (CH)	38.97 ± 48.17 [123.58]	23.4 ± 28.92 [123.58]	76.57 ± 10.64 [13.89]	0.83 ± 1.79 [214.7]	8.02 ± 3.97 [49.44]	5.05 ± 4.07 [80.47]	2.18 ± 4.09 [187.35]
Barranquilla (CO)	157.1 ± 174.28 [110.93]	12.33 ± 13.68 [110.93]	93.97 ± 5.23 [5.56]	1.68 ± 10.16 [603.23]	32.8 ± 1.49 [4.54]	27.98 ± 0.98 [3.5]	25.17 ± 1.03 [4.1]
Medellin (CO)	442.18 ± 404.89 [91.57]	17.45 ± 15.98 [91.57]	69.37 ± 7.55 [10.89]	0.85 ± 2.38 [280.93]	22.89 ± 1.48 [6.49]	22.1 ± 1.43 [6.45]	21.52 ± 1.38 [6.42]
Bogota (CO)	8.95 ± 18.7 [208.85]	18.00 ± 37.59 [208.85]	88.58 ± 5.24 [5.92]	2.47 ± 5.21 [210.78]	15.02 ± 0.84 [5.61]	14.4 ± 0.84 [5.83]	13.8 ± 0.83 [6.04]
Cali (CO)	873.92 ± 751.6 [86]	11.29 ± 9.71 [86]	sd	1.93 ± 4.74 [245.52]	24.52 ± 1.14 [4.67]	23.8 ± 1.09 [4.59]	23.15 ± 1.06 [4.59]
Leticia (CO)	299.28 ± 213.04 [71.19]	13.29 ± 9.46 [71.19]	87.62 ± 5.2 [5.94]	5.41 ± 11.68 [215.81]	26.92 ± 1.47 [5.45]	26.37 ± 1.41 [5.35]	25.74 ± 1.32 [5.12]

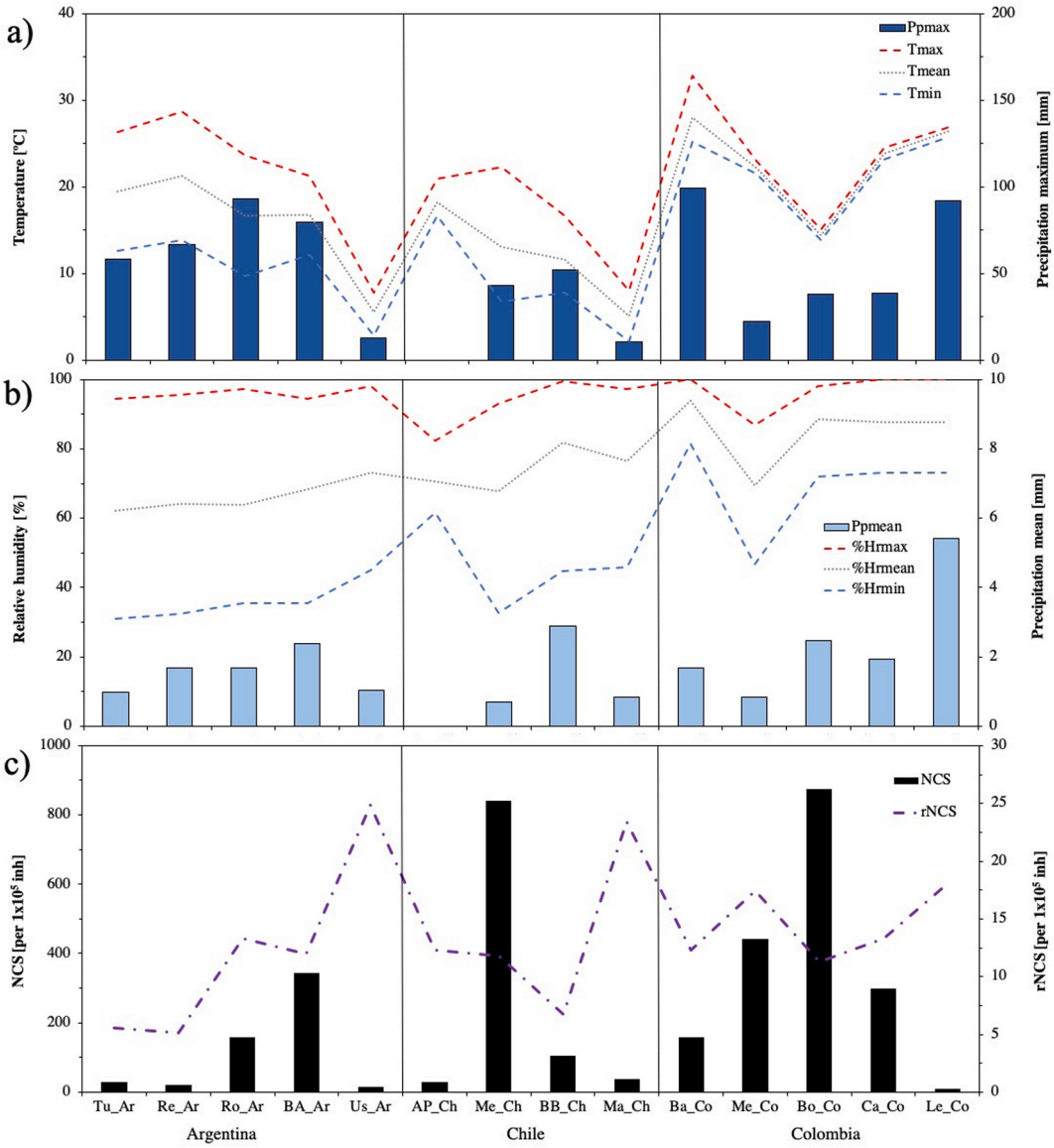

Fig. 2. Relation of climatological variables and COVID-19 cases. a) Temperature (°C, max, mean and min, dash line) and maximum precipitation (mm, blue bars). b) Relative humidity (%, max, mean and min, dash line) and mean precipitation (mm, sky blue bars). c) New cases with symptoms (NCS, black bars) and rate of new cases with symptoms per inhabitants (rNCS, dash-dotted line). (For interpretation of the references to colour in this figure legend, the reader is referred to the Web version of this article.)

climate code: ET), characterised by sub-freezing mean annual temperatures, large annual temperature ranges, and moderately low precipitation [45].

During the sampled period, a sustained increase in T_{mean} with an anomaly of 76% was observed throughout Chile (Fig. 2a). The Pp in Metropolitana was ~50.9 mm; however, in the north of the country (Arica y Parinacota), the Pp was around 0.8 mm (Table 3, Fig. 2a–b). Biobío had an average rainfall deficit of <38%, whereas in South Patagonia, the deficit reached 9% in Magallanes. In summary, the sampled period was the 2nd warmest year in 60 years, being 0.84 °C warmer than the 1961–1990 climatological average and 0.6 °C warmer than the 1981–2010 average. In Arica y Parinacota it was the 2nd rainiest year in 60 years with 7.8 mm of rainfall accumulated. In Metropolitana, the fall and spring were driest in the last 60 years and winter (June) the rainiest since 2005, accumulating 110.1 mm like Biobio (Table 3), which accumulated 344.8 mm. In winter a moderate to light drought remained, as was the case with the Magallanes (Fig. 2a). Finally, in this region rains were registered only in spring, where it rained up to 66.6 mm and it was the rainiest season since 2008.

The variance was analysed using the coefficient of variation (CV) (Table 3). The low dispersion in temperatures for the Colombia sites did not exceed 6%. Magallanes and Ushuaia, which correspond to the southernmost localities, had the greatest dispersions in T_{max},

T_{min}, and T_{mean}, with CV > 110% and >70%, respectively (Table 3). In Metropolitana site, Concepción, Tucumán, Resistencia, Rosario, and Buenos Aires were typical of the seasonal pattern. The T_{min}, T_{mean}, and CV values were between 43%–68% and 24%–35% for the sites in Argentina and Chile, respectively. Exceptions were Arica y Parinacota, which have low dispersions, with CV for temperatures of 13 %–15%, located in a region of dry climate during most of the year. In the case of daily Pp, for all sites, there was a prevalence of absence of rain, so the variance is expected to be high, given by the extreme values. As for the Hr, the CV showed that the Colombian sites, the Chilean sites Arica y Parinacota, BioBio, and Magallanes have values <14%, characteristic of their relatively uniform climatic conditions during the year (Table 3). The other group corresponded to Buenos Aires, Metropolitana, Resistencia, and Ushuaia, which showed variations between 17% and 27%. Finally, those with variations greater than 36% were Tucumán and Rosario.

3.2. Peaks of COVID-19 cases and the climatic conditions associated

The new cases with symptoms (NCS) were the cases were highest in the capitals of the selected countries (Fig. 2c) which is related to the socio-demographic characteristics (Table 5). However, the rate of new cases with symptoms per inhabitants (rNCS), seem to have a different distribution (Fig. 2c, dotted line).

Firstly, the evolution of 7rNCSma was analysed focusing on their peaks (Fig. 3). In the case of Argentina, an early evolution of cases was noticed in Buenos Aires, finding three considerable 7rNCSma peaks between the end of July and the end of August (they are softened in Fig. 3 due to the scale used), when temperature and Pp were minimal, due to the winter season. Coincidentally, 2020 was the year in which the average was lower (1981–2010). The maximum rate registered was 33 cases × 105 inhab. Likewise, late peaks were detected for Rosario, Tucumán, and Resistencia in late September and early October, with a maximum rate of 67 cases, 35 cases, and 17 cases × 105 inhab., respectively. In these months, an increase in temperature and rainfall is expected. Particularly, in Tucumán and Resistencia, the temperature was higher than the mean and the Pp was lower. On the other hand, in Rosario, both variables were higher than the mean.

Moreover, Ushuaia recorded its maximum peak (124 cases × 105 inhab.) at the beginning of November (Fig. 3), when temperatures were on the rise (and were higher than the 1981–2010 mean) and rains showed a marked decline (Pp was lower than the mean in November).

According to Chile, the first peak was reached in June in the Metropolitan Region, with a rate of 74 cases per 1 × 105 inhab., followed by Arica y Parinacota for the month of July, with 53 cases per 1 × 105 inhab. Magallanes displayed the highest value of the period with a rate of 104 cases per 1 × 105 inhab. in the month of October., and finally, In the case of Biobío, values did not show a sharp increase with an evident peak (Fig. 3).

When Colombia is considered, the first peak was reached in the first week of May in Leticia with a maximum rate of 140 cases × 105 inhab., which is a particularly humid city that encounters rains throughout the year and the temperature does not have much variation. An increase in cases was observed from the second week of April, reaching the highest in the first week of May and then

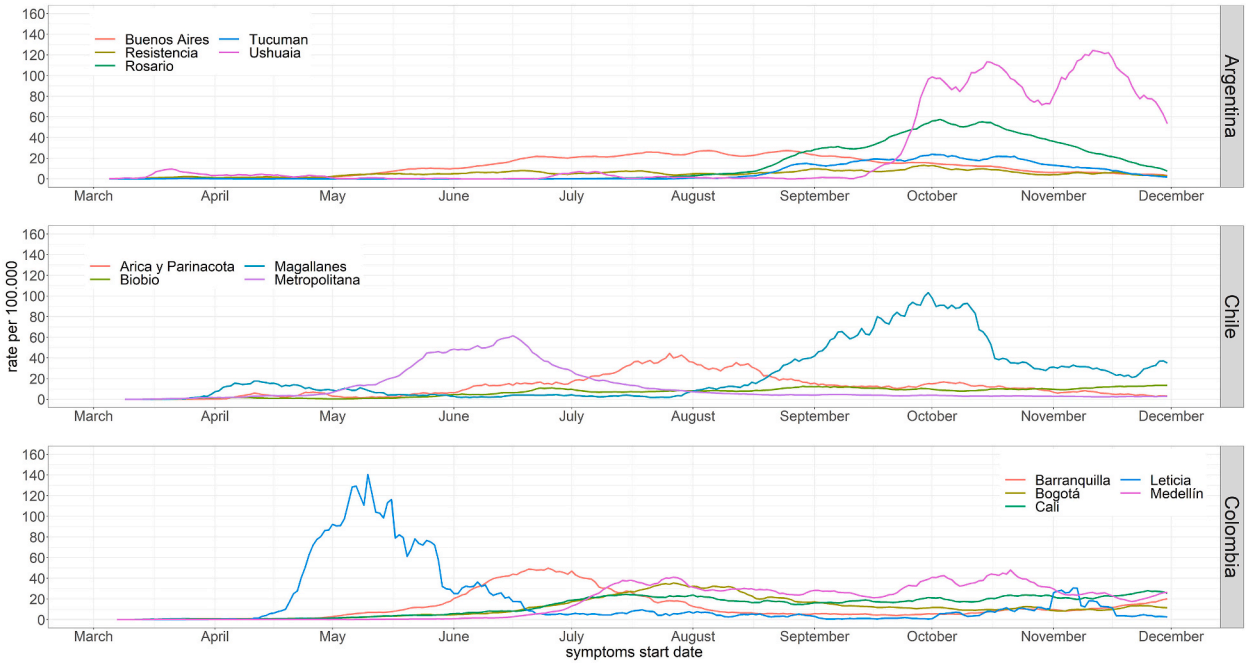

Fig. 3. 7-Day moving average rates of confirmed cases per 1 × 10^5 inhab. (7rNCSma) by date of onset of symptoms (Argentina and Colombia) and by date of confirmation (Chile) for the sites analysed from March to November 2020. Colour lines represent a site for each country. (For interpretation of the references to colour in this figure legend, the reader is referred to the Web version of this article.)

declining (Fig. 3). There was a surge again in the middle of the month, maintaining high reports of cases until the second week of June. After a considerable drop in the report was observed, reported cases remained low until the first week of November when a new peak was observed which was well below the first peak. The second peak occurred in Barranquilla with an increase in cases in mid-June and was maintained until early July during a dry season. The third peak was seen in Bogotá at the end of July and was consistent until the beginning of August, periods of low temperature. In Cali, cases escalated in the third week of June until the beginning of August and remained almost constant, rising slightly again in late November. The next peak was evident in Medellín around mid-July. Later, in October, cases surged again in the first week of the month with a brief decrease in the second week, which increased again in the third week of the month and was maintained almost until the end of the month (Fig. 3).

3.3. Link between climatic variables and COVID-19

Spearman correlations calculated between cases: rNCS, 7rNCSma, 14rNCSma, 7rNCSL and 14rNCSL and the meteorological variables per site are summarised in Table 4 (Table Supp 2) at both 5 and 1% level of significance and they vary according to the place and the variable studied. In Argentina, correlations between meteorological variables for rNCS by dates of onset of symptoms, moving averages, and lags were indirect and significant between COVID-19 cases and Hr (ρ −0.56 to −0.63) in Tucumán. A greater correlation stood out for rates by dates of onset of symptoms and with 14rNCSL. Correlations with all temperatures were direct (ρ 0.17–0.50) and significant (greater for the date of onset of symptoms and moving averages than for lags). Correlations between T_{min} and the dates of onset of symptoms and lags were not significant. In Resistencia, correlations with Hr were indirect and significant for rates by dates of onset of symptoms, 14rNCSma and 14rNCSL (ρ −0.13 to −0.2). Indirect and significant correlations were also found between all Temperatures with lags and dates of onset of symptoms (ρ −0.15 to −0.29). The highest correlations were presented with both lags for the three variables. In Rosario, Hr presented indirect and significant correlations (ρ −0.39 to −0.46). In addition, direct and significant correlations were found for T_{max} with the moving averages (ρ 0.13–0.28) and for the T_{mean} with 14rNCSma (ρ = 0.22). Correlation with Hr was not significant in Buenos Aires. All Temperatures were indirect and significant (ρ −0.56 to −0.75), being the strongest for 14rNCSL and registering the highest absolute values of ρ in comparison with other sites. In Ushuaia, as in the rest of the Argentine sites analysed except Buenos Aires, Hr was indirectly and significantly correlated (ρ −0.28 to −0.38). Similarly, as in Tucumán and Rosario, direct and significant correlations were observed with all Temperatures. These values were higher for T_{max} and T_{mean} (ρ 0.29–0.47) than for T_{min} (ρ 0.17–0.3). In summary, correlations between COVID-19 cases and Hr were indirect and significant at all sites (ρ −0.13 to −0.63), except in Buenos Aires. Strongest correlations were obtained in Tucumán and next in Rosario. The correlations between the cases and all temperatures were direct and significant in Tucumán, Rosario, and Ushuaia (ρ between 0.13 and 0.50) being the most robust for T_{max} with moving averages in Tucumán and T_{mean} with moving averages in Ushuaia, followed by Tucumán. In Resistencia and Buenos Aires these correlations were indirect and significant (ρ between −0.15 and −0.75), making Buenos Aires the strongest correlated of all sites. Correlations between COVID-19 cases and Pp were not significant at all sites and presented $\rho < 0.1$.

In Chile, with a significance of 1%, there was a direct and significant correlation with Hr, but not with variables related to temperature for the case of Arica y Parinacota. These are inverse correlations with significant values close to −1, regardless of whether the calculation was made with confirmation dates or with moving averages or lags, which highlighted that the highest correlation values were found with T_{max} (ρ −0.83 to −0.85). In the Metropolitana site, there was also a direct and significant correlation with Hr. All temperatures presented inverse and significant values, but with values of ρ lower than those obtained for Arica y Parinacota, also identifying the highest values in T_{mean} with fluctuations of ρ between −0.66 and −0.81. Pp values were close to 0 and significant (ρ −0.29 to −0.34), given the low amount of rainfall at this site. In Biobío, the directionality of the correlation with Hr and all

Table 4
Values of Spearman's correlation coefficient (ρ. rho) to the correlation between dependent variables: rates of confirmed COVID-19 cases (RCC) moving average 7-days and independent (meteorological data). Nd, non-data.

Site	%Hr	PP	Tmax	Tmean	Tmin
Tucumán (AR)	−0.56**	−0.01	0.42**	0.33**	0.17**
Resistencia (AR)	−0.17**	−0.05	−0.09	−0.07	−0.04
Rosario (AR)	−0.43**	0.04	0.2**	0.14*	0.06
Buenos Aires (AR)	−0.07	−0.07	−0.61**	−0.63**	−0.59**
Ushuaia (AR)	−0.36**	−0.03	0.42**	0.37**	0.24**
Arica y Parinacota (CH)	0.33**	nd	−0.85**	−0.83**	−0.67**
Metropolitana (CH)	0.65**	0.33**	−0.71**	−0.81**	−0.67**
Bíobío (CH)	−0.22**	−0.01	−0.24**	−0.23**	−0.19**
Magallanes (CH)	−0.35**	−0.12*	0.16*	0.22**	0.16**
Barranquilla (CO)	0.33**	0.13*	0.22**	0.32**	0.14*
Medellin (CO)	0.23**	−0.07	−0.34**	−0.34**	−0.35**
Bogota (CO)	0.12	0.07	−0.39**	−0.41**	−0.42**
Cali (CO)	–	−0.09	−0.19**	−0.22**	−0.23**
Leticia (CO)	0.09	0.15*	−0.05	−0.07	−0.06

* Significant 5%.
** High significant 1%.

Table 5
Socio-demographic characterisation of study sites. Databases provided by different ministries: Argentina (INDEC). Chile (INE). Colombia (DANE). GINI index estimated to 2015 [48]. New cases with symptoms (NCS) and rate of new cases with symptoms per inhabitants rNCS.

Sites	COVID-19 data		Population index*			Socio-economic index		
	NCS	rNCS	x 10^3 inh	δ (inh km^{-2})	Pop. (>60 years) (%)	Monetary Poverty** (%)	Masculinity Index* (%)	Gini†
Tucumán (AR)	8461	1541.5	606	6.098.5	13.3	43.5	90.7	0.416
Resistencia (AR)	5541	1417.6	443	112.0	10.7	53.6	93.2	ND
Rosario (AR)	44247	3691.8	1291	5.571.0	16.6	38.3	91.9	0.400
Buenos Aires (AR)	95545	3.305.9	3076	14.450.8	21.7	16.5	85.2	0.432
Ushuaia (AR)	3923	6887.8	57	6.1	6.4	sd	104.7	nd
Arica y Parinacota (CH)	7593	3358.7	226	13.4	15.4	8.4	99.2	0.440
Metropolitana (CH)	229561	3227.4	7.113	462	15.4	5.4	94.8	0.523
Bíobío (CH)	28677	1842.0	1.557	65.0	16.8	12.3	93.1	0.465
Magallanes (CH)	10640	6389.1	167	0.1	16.9	2.1	104.9	0.448
Barranquilla (CO)	43203	3390.5	1.274	8274.0	25.7	25.6	92	0.462
Medellin (CO)	121600	4799.8	2.533	5820.0	18.2	24.4	89.1	0.484
Bogota (CO)	240329	3103.4	7.744	4907.0	25.3	27.9	91.9	0.513
Cali (CO)	82301	3653.6	2.253	4382.0	30.4	21.9	87.5	0.465
Leticia (CO)	2462	4950.0	50	7.8	5.6	sd	98.3	nd

* Argentina: INDEC. population projection to 2020 based on the National Population. Household and Housing Census 2010; Chile: INE. Population and Housing census 2017; Colombia: DANE. National Population and Housing census 2018.

** Argentina: INDEC. Permanent Survey of Households 2019; Chile: Ministry of Social Development. National Socioeconomic Characterization Survey (CASEN) 2017; Colombia: DANE. Monetary poverty and extreme monetary poverty technical annex 2019

† Argentina: INDEC. Permanent Survey of Households 2019; Chile: Gini index estimated in 2015[48]. Colombia: DANE. Monetary poverty and extreme monetary poverty technical annex 2019.

temperatures were inverted and significant and highest values were detected in T_{max} with (ρ −0.17 to −0.36). Magallanes presented inverse and significant correlations for Hr and Pp, similar to Biobío (Table 4). However, temperatures did not present stable values when studied by confirmation dates, moving averages, or lagged, since although they presented positive correlation values, they were not significant in all measurements.

In Colombia, correlations between meteorological variables for rates, moving averages, and lags were direct and the strongest in Barranquilla with Hr (ρ 0.28–0.36), T_{mean} (ρ 0.27–0.38), and T_{max} (ρ 0.18–0.28). There was no significant correlation between T_{min} and 14rNCSma. Medellin had a direct correlation between Hr and rNCS, 7rNCSma and 14rNCSma (ρ 0.23–0.29). All temperatures followed the same correlation but inverse (ρ −0.33 to −0.38). In contrast to Barranquilla and Medellin, Hr in Bogotá showed significant correlations only for rNCS, 7rNCSL and 14rNCSL (ρ 0.16–0.2). The temperature was similar to that in Cali and Barranquilla, with an inverse relationship between the rate, moving averages, and lags with respect to all Temperatures (ρ −0.35 to −0.46). Cali showed a significant correlation between rNCS, moving averages, and lags with respect to all temperatures (ρ 0.14–0.31), while temperatures had an inverse correlation for all three cases. Leticia demonstrated an Hr with a positive correlation for 14rNCSL ($\rho = 0.16$). As for Pp, significant and direct correlations (ρ 0.10) were only observed for the 14rNCSma. There were no significant correlations with all temperatures for 14rNCSma by this site (Table 4).

In summary, an indirect and significant correlation (p value <0.01) was found in Magallanes, as well as in most sites in Argentina (except Buenos Aires) between Hr and rNCS. With the same variables, a direct and significant correlation ($p < 0.01$) was found for Arica y Parinacota, Metropolitana, Barranquilla, and Medellín. Indirect and significant correlations ($p < 0.05$) found in BioBio, Buenos Aires, Bogotá, and Leticia were not significantly correlated. This variable was not analysed for Cali because the data were discarded due to errors. Pp presented significant ($p < 0.01$) and direct correlations in Metropolitana and inverse correlations in Magallanes. Correlations were significant ($p < 0.05$) and direct in Barranquilla and Leticia. Significant inverse correlations ($p < 0.01$) with all temperatures were obtained for all sites in Chile (except Magallanes), as well as for Medellín, Bogotá, and Cali in Colombia and Buenos Aires in Argentina. Inversely, direct and significant correlations ($p < 0.01$) were found in Tucumán and Ushuaia, only with T_{max} in Rosario, and T_{max} and T_{mean} in Barranquilla. Finally, the sites of Leticia and Resistencia were not significantly correlated.

The CVs of the NCS and rNCS were the greatest for Leticia, followed by Ushuaia, Tucumán, Rosario, Metropolitana, Magallanes, and Barranquilla. This scattering behaviour was observed for smaller sites, which nevertheless had different climatic characteristics. Based on these results, an exploration of the link between NCS and rNCS and environmental variables at all sites was carried out using PCA (Fig. 4 a). PC1 explained that 45.6% of the total variability was defined as the thermal variability mainly associated with equatorial sites. Most of the sites were related to the hottest sites with temperatures above 23 °C and low CV. Magallanes and Ushuaia had similar but opposite behaviours to other sites. PC2 (22.6%) was defined as greater variability in precipitation and relative humidity that was associated with a higher rate of NCS. This was reflected in most of the sites in Argentina (with the exception of Ushuaia) and in the Central North of Chile (Metropolitana, Arica y Parinacota).

3.4. Link between socioeconomic and demographic variables and COVID-19

The maximum rNCS for the entire period (March to November) was registered in the three cities that were less populated (Ushuaia,

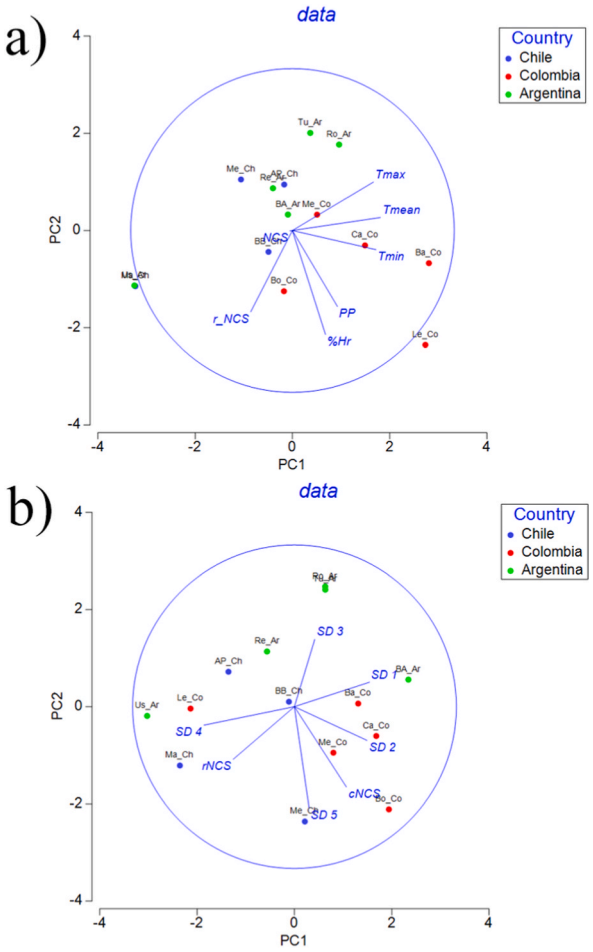

Fig. 4. Principal component analysis that linking COVID-19 data (NCS and rNCS) and (a) meteorological variables (Relative humidity (Hr, %), Temperature (°C), Precipitation (Pp, mm). (b) sociodemographic data (see variable description SD in Table 6) by sampled sites in each country (Argentina, Chile and Colombia).

24.9; Magallanes, 23.4; and Leticia, 18.0). In relation to population density, half of the sites have more than 1000 inhabitants per square kilometre (inhabs km^{-2}), of the remaining sites, two have densities between 100 and 1000 inhabitants km^{-2} and five less than 100 inhabs km^{-2}. The most densely populated site is Buenos Aires, which has more than 14,000 inhabs km^{-2}. The maximum rNCS was observed in the two cities with less population density (Ushuaia and Magallanes) (Table 5).

The most and least populated sites under study were in Colombia (Bogotá and Leticia) with more than seven million and less than 50,000 inhabitants, respectively (Table 5). Cali, Bogotá, Barranquilla and Buenos Aires had the highest percentages of people aged 60 years or more with respect to age groups of urban population. Nine sites had less than 18% of the population aged 60 and over, while Ushuaia, the southernmost city, had 6%. The highest masculinity index (over 100%) occurred at two sites with the lowest density and

Table 6
Values of Spearman's correlation coefficient (ρ. rho) to the correlation between dependent variables. rates of confirmed COVID-19 cases (RCC). moving average 7-days. and independent sociodemographic variables. SD. socio-demographic variables to principal component analysis. NCS: New cases with symptoms. rNCS: rate of new cases with symptoms

Spearman rank	NCS	rNCS
Pop (h)	0.956**	−0.401
δ (h km^{-2}) (SD1)	0.511**	−0.363
Pop. (>60 years) (%) (SD2)	0.659**	0.033
Monetary Poverty (%) (SD3)	−0.291	−0.589**
Masculinity Index (%) (SD4)	−0.593**	0.324
GINI (SD5)	0.717**	−0.017

** high significant 1%

quantity of population—Magallanes (Chile) and Ushuaia (Argentina), while the lowest masculinity indices were in Buenos Aires (Argentina) with 85% and Cali 87% (Colombia). Eleven of the sites analysed had women preponderance (Table 5).

Four sites had more than a quarter of their poor population, five with poverty levels between 10% and 25%, and four below 10%. The site with the lowest proportion of poverty was Magallanes (Chile), while the city with the highest proportion was Resistencia (Argentina), with more than half of its population poor (Table 5).

Based on results obtained with socio-economic and demographic variables measured at the different sites studied an exploratory analysis was carried out to determine possible associations with the COVID-19 data of RCC (NCS and rNCS) using the Spearman correlation (Table 6). It was observed that rNCS had a significant negative correlation with monetary poverty, while NCS had significant positive correlations with the number of inhabitants (Pop h), population aged 60 years and older. (Pop. ⩾ 60 years, %), GINI index and negative with the masculinity index. This allowed us to observe that the greatest number of NCS was in sites with a larger population size, a higher percentage of adults over 60 years of age, a lower masculinity index, and a higher GINI value (Table 6).

Sites with higher NCS, population, population aged 60 years and over, lower % of masculinity, and higher GINI, such as Bogotá, Cali, Medellin, Metropolitan, Buenos Aires, and Rosario have formed a group with a similar association between social variables and COVID-19. On the other hand, at the opposite extreme with lower NCS, population, population 60 years old and over, a higher % of masculinity, and lower GINI were Leticia, Arica y Parinacota, Tucumán, Resistencia, and Ushuaia. In the middle of these values were sites such as Barranquilla, Biobío, and Magallanes.

Based on these results, relationships between the sites were explored using PCA (see Fig. 4b). In the first instance, all analyses that included the variable 'population size' concentrated all the variation in a single factor, not allowing a clear discrimination of sites. One of the results that showed a similar pattern to results obtained through correlations was the one that used all the variables except 'population size' and in that case, population density was used. This PCA run yielded two axes that explained 69.9% of the observed variation. The PC1 with 40.4% was defined as '*population status*' and explained that the rate of COVID-19 cases (rNCSC) increased in the population older than 60 years, in men, and in more populated places. This was reflected in sites such as Metropolitana, Buenos Aires, and most of the sites in Colombia, with the exception of Leticia. On the other hand, PC2 (29.5%) would explain that the greater the income inequality; the greater the poverty the greater the number of positive cases of COVID (NCS).

3.5. *Link between climatic, socioeconomic and demographic variables and COVID-19*

Non-metric multidimensional scaling with environmental fitting analysis showed a well-adjusted stress = 0.09 (Fig. 5). Except for precipitation, all meteorological variables showed significant relationships with NCS and rNCS and supported the PCA ordination with similar site groupings. Positions of sites sampled in the nMDS based on COVID-19 and socioeconomic and demographic data showed that, along the nMDS horizontal axis, the following were distributed following horizontal gradients of temperature: max, mean, and min. These three predictors had significant effects. Big site assemblages were distinct from those of the other sites sampled. The central-northeast of Argentina also clustered together and separated from the austral Patagonia sites (Magallanes and Ushuaia). Finally, a group that included two sites in Chile and another in Colombia showed an average behaviour.

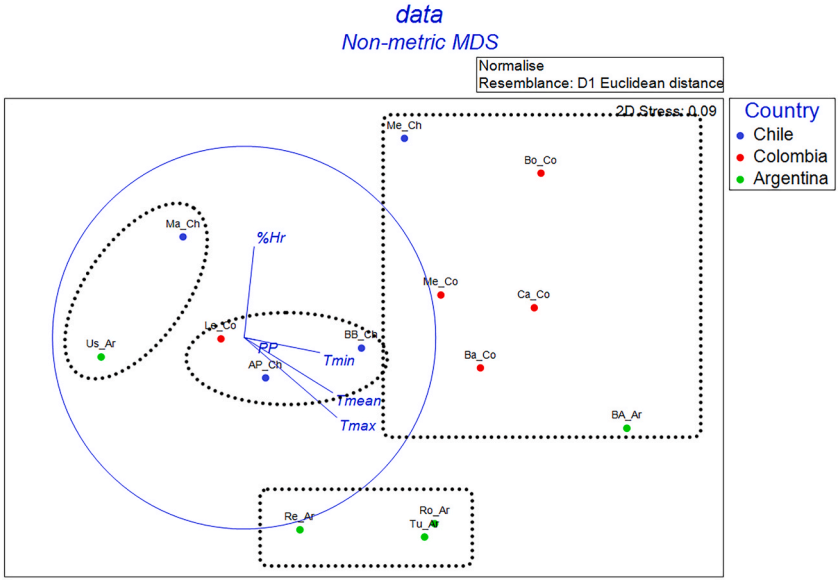

Fig. 5. Non-metric MultiDimensional Scaling ordination (nMDS) using the Bray-Curtis matrix of similarity of meteorological data, socio-demographic variables and COVID-19 (NCS and rNCS). Summary of all dimensions where some sites are most influenced by meteorological and others sociodemographic variables and/or a combination between them.

4. Discussion and conclusion

4.1. Climatic variability forcing COVID-19 cases in South America

The spread of the new COVID-19 virus was associated with latitude and longitude as geographic indicators in addition to seasonal dynamics [40,49,50]. It has also been confirmed that tropical countries have been marginally affected by the SARS CoV-2 virus and that a high transmission of COVID-19 has been observed in countries with cold-dry conditions in temperate climates [51]. Recent studies have also estimated that the low number of confirmed positive COVID-19 cases seen in tropical countries can be explained by their usual hot and humid environmental conditions [52]. In fact, they have also found that countries experiencing high absolute humidity above 10 gm-3 could see a slowdown in COVID-19 transmission in a short time. Other studies also confirmed that temperature and humidity were factors affecting the number of deaths from COVID-19 in Wuhan, China [53]. In Mexico, the regional onset of the pandemic occurred in tropical climate zones at average temperatures around 25.95 °C and average rainfall around 8.74 mm. However, in dry climates it arose earlier because of lower temperatures and higher rainfall (20.57 °C and 20.87 mm respectively) than those observed in tropical climates [54].

In particular, considering the simultaneous correlations, certain similarities and differences were perceived in the Bolaño-Ortiz et al. (2020) study [15]. They evaluated the spread of SARS-CoV-2 in ten Latin American and Caribbean cities during the first two months in 2020 (April–May), which coincides with our study in three capitals: Bogotá (Colombia), Santiago (Chile) (included in Metropolitana site), and Buenos Aires (Argentina). In the case of the Metropolitana site, both studies found negative and significant simultaneous correlations with temperatures and positive and significant correlations with Hr. We also found a significant correlation with Pp, similar to that in Bolaño-Ortiz et al. (2020) study [15].

Likewise, for Bogotá, results were in line with Hr and Pp, which were not significant. However, studies conducted in Brazil [55] found that higher T_{mean} and average Hr favoured the transmission of COVID-19, unlike reports from colder countries or periods of time under cold temperatures, which was when the highest number of COVID-19 cases were present. This was especially true for the cities of São Paulo and Rio de Janeiro, which are cities of great importance. São Paulo is the main economic destination for job seekers and investors, and Rio de Janeiro is the most important tourist destination in the country. An analysis of the evolution of COVID-19 transmission cases in these sites deserves special attention due to their economic relevance as well as their population density; Tosepu et al. (2020) [56] have found that only temperature average (°C) was significantly correlated with covid-19 pandemic in Jakarta. This correlation is in line with the correlation present in previous research showing the relationship between meteorological transmission and respiratory syncytial virus [57] and SARS [58]. Temperature is also an environmental factor in the COVID-19 outbreak in China, and the regression equation shows how temperature, Hr, and wind speed affect the transmission of SARS [23]. Despite the weather, high COVID-19 cases in Jakarta are also caused by the extremely high mobility of people. As the capital city of Indonesia, Jakarta is the main economic destination for job seekers. The population density of Jakarta is also very high, which allows rapid transmission of COVID-19 [55,56]. Finally, for Buenos Aires our results agree with Bolaño-Ortiz et al. 2020 [15], who also had non-significant correlations with Hr. However, correlations between temperature and Pp differed.

The first COVID-19 peaks were found in main sites where airports with the highest passenger traffic were located: in the case of Chile, Metropolitana, and in Argentina, Buenos Aires. Moreover, in Colombia, the first peak was observed in Leticia, although no significant correlations with climatic variables were found (except for Pp) for that site. This indicates that the increase in the rate of COVID-19 cases can be explained by other variables, such as social and environmental factors, whose influence can be related to the location of the site on the border with Brazil. In addition, in those sites that are close to the borders with other countries (Leticia, with Brazil and Arica y Parinacota with Peru), correlations found can be explained by the flow of people rather than by meteorological variables. Therefore, a significant correlation with temperature was observed in Arica y Parinacota, but not in Leticia. In addition, the three main sites (Buenos Aires, Bogotá, and Metropolitana) showed a higher (and negative) correlation with temperature compared to other meteorological variables. The sites in southern South America (Magallanes and Ushuaia) showed the opposite behaviour to Arica y Parinacota (northern Chile) in terms of correlations between the rate of COVID-19 cases and Hr and temperatures. Therefore, it is highly probable that high altitude reduces the infection rate of COVID-19 but not case-fatality, as was shown in our study [59–61].

Finally, it is worth noting that correlations found gave us an idea of the relationship between meteorological variables and the rate of COVID-19 cases; with a prevalence of the behaviour of simultaneous and previous values of temperature and relative humidity, however, they do not indicate causality. The current global climate change scenario puts researchers on alert about future pandemics and the need to stimulate multidisciplinary studies for the resilience of humanity, especially in regions where climate variability and socio-economic conditions play a significant role.

4.2. Socioeconomic and demographic variability as a driving force of COVID-19 cases in South America

Climatic, environmental, socio economic and demographic factors such as cultural factors, population density, and other factors can influence the transmission of the virus in Latin America and the Caribbean region [15,62]. Bolaño-Ortiz et al. (2020) [15] have studied the relationship between meteorological and social variables and COVID-19 morbidity and mortality, considering the GINI index estimated to 2015 [61], urban poverty rate, and urban extreme poverty rate to describe social inequity. Interestingly, they have suggested that income inequality and poverty levels are correlated with the spread of COVID-19. However, these studies should be conducted for a longer period of time and consider the lockdown status for each city. Buenos Aires and Bogotá applied a full lockdown, while Santiago had some areas under lockdown.

In relation to the work of Bolaño-Ortiz et al. (2020) [15], in our case, the variable that showed significant correlations with the

socio-economic variables was NCS, not the NCS rate. Similarly, the GINI index had a positive correlation with NCS (0.71). We did not find significant correlations with the poverty index analysed, but with the percentage of adults aged 60 years and older and with the masculinity index, which were inconsistent with the findings of Bolaño-Ortiz et al. (2020) [15]. It was observed that the highest number of NCS was found in places with a larger population size, a higher percentage of adults aged 60 years and older, a lower masculinity index, and a higher GINI value. However, unlike the GINI index, for example, in similar studies in cities in France or Japan, the age structure of the population has not been found to have definitive significance in the number of cases observed [31]. On the other hand, studies on a global scale have found that total cases of COVID-19 are correlated with the percentage of adults over 65 years of age [63,64].

These results seem to indicate that, at least in our case, demographic variables were more significant factors in relation to COVID-19 cases than socio-economic ones. The population density is the most significant factor that increases in contact between people, and therefore, the number of cases [65,66]. Our results support the hypothesis that epidemiological studies of COVID-19 have, to date, offered mixed results regarding the meteorological sensitivity of the virus and the disease. COVID-19 transmission dynamics in 2020 appear to have been related to sociodemographic factors and controlled primarily by government interventions rather than meteorological factors.

The interplay and interactions between the climatic, socio economic and demographic variables and COVID cases and rates are complex. We performed an exploratory analysis with some limitations of data access and methods. Future studies with longer data series and the inclusion of other determinants that influence the spread of the virus (i.e., public policies, health and economic measures, and the response of the public health sector) will allow a better understanding of the role of climatic and non-climatic factors in the development of the COVID-19 epidemic in these latitudes. Due to the rapid evolution of the COVID-19 pandemic, multidisciplinary approach is essential to address different aspects related to the social health determinants of COVID-19 morbidity in South America. We hope our findings will encourage new groups from different disciplines and sciences to jointly work in order to understand the current state of COVID-19 transmission in our region and its imminent evolution.

Author contribution statement

Gilma Mantilla Caicedo: Conceived and designed the experiments; Performed the experiments; Analysed and interpreted the data; Contributed reagents, materials, analysis tools or data; Wrote the paper.

Matilde Rusticucci, Martín Díaz, Silvia Fontán, Francisco Chesini: Conceived and designed the experiments; Analysed and interpreted the data; Wrote the paper.

Solange Suli, Verónica Dankiewicz, Salvador Ayala: Performed the experiments; Analysed and interpreted the data; Contributed reagents, materials, analysis tools or data; Wrote the paper.

Alexandra Caiman Peñarete: Analysed and interpreted the data; Wrote the paper.

Diana Lucia Jiménez Buitrago: Analysed and interpreted the data; Contributed reagents, materials, analysis tools or data; Wrote the paper.

Luis Reinaldo Barreto Pedraza: Contributed reagents, materials, analysis tools or data.

Facundo Barrera: Conceived and designed the experiments; Performed the experiments; Analysed and interpreted the data; Wrote the paper.

Data availability statement

Data included in article/supplementary material/referenced in article.

Funding

This research was funded partially by Centre for Climate and Resilience Research (CR)2, (ANID/FONDAP/15110009) (FB), FONDECYT 3180307 (FB) and CONICET PIP0137 (MR). SS and VD were supported by a doctoral scholarship from CONICET; SA was supported by a doctoral scholarship from ANID National PhD. Scholarship No. 21191111.

Declaration of Competing Interest

The authors declare that they have no known competing financial interests or personal relationships that could have appeared to influence the work reported in this paper.

Acknowledgements

This research was funded partially by Centre for Climate and Resilience Research (CR)2, (ANID/FONDAP/15110009) (FB), FONDECYT 3180307 (FB) and CONICET PIP0137 (MR). SS and VD were supported by a doctoral scholarship from CONICET; SA was supported by a doctoral scholarship from ANID Beca Doctorado Nacional No. 21191111. Rusticucci, Mantilla, Barrera, Chesini, Fontan, Ayala, Cabrera, Caiman, Dankiewicz and Diaz participated in the Seminar: *Instruments and Methodologies for a Climate Observatory and its impact on human health* founded by Centro CELFI – CIENCIA DE LOS DATOS MINISTERIO DE CIENCIA, TECNOLOGÍA E INNOVACIÓN PRODUCTIVA developed in September 2019. Rusticucci, Chesini and Fontan are developing the workshop

ARCHITECTURE OF A NATIONAL CLIMATE AND HEALTH OBSERVATORY, founded by Agencia Nacional de Promoción de la Investigación, el Desarrollo Tecnológico y la Innovación. We also would like to thank Editage (www.editage.com) for English language editing.

Appendix A. Supplementary data

Supplementary data to this article can be found online at https://doi.org/10.1016/j.heliyon.2023.e16056.

References

[1] R. Lu, X. Zhao, J. Li, P. Niu, B. Yang, H. Wu, W. Wang, H. Song, B. Huang, N. Zhu, et al., Genomic characterisation and epidemiology of 2019novel coronavirus: implications for virus origins and receptor binding, Lancet 395 (2020) 565–574, https://doi.org/10.1016/S0140-6736(20)30251-8.
[2] N. Srivastava, P. Baxi, R.K. Ratho, S.K. Saxena, Global trends in epidemiology of coronavirus disease 2019 (COVID-19), in: Coronavirus Disease 2019 (COVID-19: Epidemiology, Pathogenesis, Diagnosis, and Therapeutics, first ed., Springer, 2020, pp. 9–21, https://doi.org/10.1007/978-981-15-4814-7_2.
[3] N. Zhu, D. Zhang, W. Wang, X. Li, B. Yang, J. Song, et al., A novel coronavirus from patients with pneumonia in China, 2019, N. Engl. J. Med. 382 (2020) 727–733, https://doi.org/10.1056/NEJMoa2001017.
[4] D. Crawford, The Invisible Enemy: a Natural History of Viruses, OUP Oxford, 2002.
[5] Van Regenmortel, MHV, Viruses are real, virus species are man-made, taxonomic constructions, Arch. Virol. 148 (2003) 2481–2488, https://doi.org/10.1007/s00705-003-0246-y.
[6] T. Yadav, S.K. Saxena, Transmission cycle of SARS-CoV and SARS-CoV-2, in: S. Saxena (Ed.), Coronavirus Disease 2019 (COVID-19). Medical Virology: from Pathogenesis to Disease Control, Springer, Singapore, 2020. https://doi-org.dti.sibucsc.cl/10.1007/978-981-15-4814-7_4.
[7] S.K.P. Lau, J.F.W. Chan, Coronaviruses: emerging and re-emerging pathogens in humans and animals, Virol. J. 12 (2015) 209, https://doi.org/10.1186/s12985-015-0432-z.
[8] N. Madhav, B. Oppenheim, M. Gallivan, P. Mulembakani, E. Rubin, N. Wolfe, Pandemics: risks, impacts, and mitigation, in: Improving Health and Reducing Poverty, third ed.Disease Control Priorities, Vol. 9., The World Bank, 2017 https://doi.org/10.1596/978-1-4648-0527-1_ch17.
[9] Y. Muthuraman, I. Lakshminarayanan, A review of the COVID-19 pandemic and its interaction with environmental media, Environ. Chall. 3 (2021), 1000040, https://doi.org/10.1016/j.envc.2021.100040.
[10] WHO, Weekly Operational Update on COVID-19 - 30 November 2020, World Health Organization, 2020. www.who.int/publications/m/item/weekly-operational-update—30-november-2020.
[11] PAHO, COVID-19 - PAHO/WHO Response, Report 36 (30 November 2020). World Health Organization. www.paho.org/en/documents/covid-19-pahowho-response-report-36-30-november-2020.
[12] S. Altizer, R. Ostfeld, P. Johnson, S. Kutz, C. Harvell, Climate change and infectious diseases: from evidence to a predictive framework, Science 341 (6145) (2013) 514–519, https://doi.org/10.1126/science.1239401.
[13] P.J. Ward, M. Kummu, U. Lall, Flood frequencies and durations and their response to el Niño southern oscillation: global analysis, J. Hydrol. 539 (2016) 358–378, https://doi.org/10.1016/j.jhydrol.2016.05.045.
[14] S. Lin, Y. Fu, X. Jia, S. Ding, Y. Wu, Z. Huang, Discovering correlations between the COVID-19 epidemic spread and climate, Int. J. Environ. Res. Publ. Health 17 (21) (2020) 7958, https://doi.org/10.3390/ijerph17217958.
[15] T.R. Bolaño-Ortiz, Y. Camargo-Caicedo, S.E. Puliafito, M.F. Ruggeri, S. Bolaño-Diaz, R. Pascual-Flores, J. Saturno, S. Ibarra-Espinosa, O.L. Mayol-Bracero, E. Torres-Delgado, F. Cereceda-Balic, Spread of SARS-CoV-2 through Latin America and the Caribbean region: a look from its economic conditions, climate and air pollution indicators, Environ. Res. 191 (2020), 109938, https://doi.org/10.1016/j.envres.2020.109938.
[16] M. Rahman, M. Islam, M.H. Shimanto, J. Ferdous, A. Al-Nur Shanto Rahman, P. Singha Sagor, et al., A global analysis on the effect of temperature, socio-economic and environmental factors on the spread and mortality rate of the COVID-19 pandemic, Environ. Dev. Sustain. 23 (2021) 9352–9366, https://doi.org/10.1007/s10668-020-01028-x.
[17] J. Cifuentes-Faura, COVID-19 mortality rate and its incidence in Latin America: dependence on demographic and economic variables, Int. J. Environ. Res. Publ. Health 18 (13) (2021) 6900, https://doi.org/10.3390/ijerph18136900.
[18] B.D. Dalziel, S. Kissler, J.R. Gog, C. Viboud, O.N. Bjornstad, C.J.E. Metcalf, Urbanization and humidity shape the intensity of influenza epidemics in U.S. cities, Science (New York, N.Y.). 362 (6410) (2018) 75–79, https://doi.org/10.1126/science.aat6030.
[19] S. Chen, K. Prettner, M. Kuhn, P. Geldsetzer, C. Wang, T. Bärnighausen, D.E. Bloom, Climate and the spread of COVID-19, Sci. Rep. 11 (2021) 9042, https://doi.org/10.1038/s41598-021-87692-z.
[20] G.F. Ficetola, D. Rubolini, Containment measures limit environmental effects on COVID-19 early outbreak dynamics, Sci. Total Environ. 761 (2021), 144432, https://doi.org/10.1016/j.scitotenv.2020.144432.
[21] N. Islam, Q. Bukhari, Y. Jameel, S. Shabnam, A.M. Erzurumluoglu, M.A. Siddique, et al., COVID-19 and climatic factors: a global analysis, Environ. Res. 193 (2021), 110355, https://doi.org/10.1016/j.envres.2020.110355.
[22] A. Saczewska-Piotrowska, D. Piotrowski, Effects of air temperature on COVID-19 case fatality rate, Contemp. Econ. 15 (1) (2021) 53–64, https://doi.org/10.5709/ce.1897-9254.435.
[23] J. Yuan, H. Yun, W. Lan, W. Wang, S.G. Sullivan, S. Jia, A climatologic investigation of the SARS-CoV outbreak in Beijing, China, Am. J. Infect. Control 34 (4) (2006) 234–236, https://doi.org/10.1016/j.ajic.2005.12.006.
[24] J. Shaman, M. Kohn, Absolute humidity modulates influenza survival, transmission, and seasonality, Proc. Natl. Acad. Sci. USA 106 (9) (2009) 3243–3248, https://doi.org/10.1073/pnas.0806852106.
[25] B. Admou, R. Hazime, I. Brahim, A.R. El Adib, Influencing factors of SARS-Cov2 spread in Africa, J. Global Health 10 (2) (2020), 020331, https://doi.org/10.7189/jogh.10.020331.
[26] G. Bull, The weather and deaths from pneumonia, Lancet 315 (1980) 1405–1408, https://doi.org/10.1016/S0140-6736(80)92666-5.
[27] M.F. Bashir, B. Ma, Bilal, B. Komal, M.A. Bashir, D. Tan, M. Bashir, Correlation between climate indicators and COVID-19 pandemic in New York, USA, Sci. Total Environ. 728 (2020), 138835, https://doi.org/10.1016/j.scitotenv.2020.138835.
[28] F. Bloise, M. Tancioni, Predicting the spread of COVID-19 in Italy using machine learning: do socio-economic factors matter? Struct. Change Econ. Dynam. 56 (2021) 310–329, https://doi.org/10.1016/j.strueco.2021.01.001.
[29] M. Nicola, Z. Alsafi, C. Sohrabi, A. Kerwan, A. Al-Jabir, C. Iosifidis, et al., The socio-economic implications of the coronavirus pandemic (COVID-19): a review, Int. J. Surg. 78 (2020) 185–193, https://doi.org/10.1016/j.ijsu.2020.04.018.
[30] R.S. Varkey, J. Joy, G. Sarmah, P.K. Panda, Socioeconomic determinants of COVID-19 in Asian countries: an empirical analysis, J. Publ. Aff. 21 (2021), e2532, https://doi.org/10.1002/pa.2532.
[31] S. Goutte, T. Péran, T. Porcher, The role of economic structural factors in determining pandemic mortality rates: evidence from the COVID-19 outbreak in France, Res. Int. Bus. Finance 54 (2020), 101281, https://doi.org/10.1016/j.ribaf.2020.101281.

[32] Ò. Miró, A. Alquézar-Arbé, P. Llorens, F.J. Martín-Sánchez, S. Jiménez, A. Martín, et al., Comparación de las características demográficas y comorbilidad de los pacientes con COVID-19 fallecidos en hospitales españoles, en función de si ingresaron o no en Cuidados Intensivos, Med. Intensiva 45 (1) (2021) 14–26, https://doi.org/10.1016/j.medin.2020.09.002.
[33] P.M. Reyes, A. Hurtado Jaramillo, L. Rendón Rojas, Efecto de factores socio-económicos y condiciones de salud en el contagio de COVID-19 en los estados de México, Contaduría Adm. 65 (2020) 17, https://doi.org/10.22201/fca.24488410e.2020.3127.
[34] R.P. Alvarez, P.R. Harris, COVID-19 en América Latina: Retos y oportunidades, Rev. Chil. Pediatr. 91 (2) (2020) 179–182, https://doi.org/10.32641/rchped.vi91i2.2157.
[35] A. Blackman, A.M. Ibañez, A. Izquierdo, P. Keefer, M.M. Moreira, N. Schady, T. Serebrisky, La política pública frente al COVID-19: Recomendaciones para América Latina y el Caribe, Inter-American Development Bank, 2020, p. 810, https://doi.org/10.18235/0002302. Disponible en:.
[36] L.D. Acosta, Capacidad de respuesta frente a la pandemia de COVID-19 en América Latina y el Caribe, Rev. Panam. Salud Públic 44 (2020) e109, https://doi.org/10.26633/RPSP.2020.109.
[37] P. Ponce, V. Loaiza, M.D.L.C. del Río, L.B. Parra, Efecto de la desigualdad y la actividad económica en el COVID-19 en Ecuador: Un bosquejo de sus posibles determinantes económicos, sociales y demográficos, Contaduría Adm. 65 (4) (2020) 211. http://www.cya.unam.mx/index.php/cya/article/view/3044.
[38] J.C. Zevallos, C. Uriol Lescano, Letalidad y la mortalidad de Covid 19 en 60 países afectados y su impacto en los aspectos demográficos, económicos y de salud, Rev. Méd. Hered. 31 (4) (2020) 214–221, https://doi.org/10.20453/rmh.v31i4.3852.
[39] A.J. Smit, J.M. Fitchett, F.A. Engelbrecht, R.J. Scholes, G. Dzhivhuho, N.A. Sweijd, Winter is coming: a southern hemisphere perspective of the environmental drivers of SARS-CoV-2 and the potential seasonality of COVID-19, Int. J. Environ. Res. Publ. Health 17 (16) (2020) 5634, https://doi.org/10.3390/ijerph17165634.
[40] P. Duarte, E. Riveros-Perez, Understanding the cycles of COVID-19 incidence: principal Component Analysis and interaction of biological and socio-economic factors, Ann. Med. Surg. 66 (2021), 102437, https://doi.org/10.1016/j.amsu.2021.102437.
[41] J. Oksanen, F.G. Blanchet, M. Friendly, R. Kindt, P. Legendre, D. McGlinn, et al., Vegan: Community Ecology Package. R Package Version 2.5-2, Available online: https://CRAN.R-project.org/package=vegan, 2018. (Accessed 28 March 2021). accessed on.
[42] M. Charrad, N. Ghazzali, V. Boiteau, A. Niknafs, NbClust: an R package for determining the relevant number of clusters in a data set, J. Stat. Software 61 (6) (2014) 1–36, https://doi.org/10.18637/jss.v061.i06.
[43] N.M. Razali, Y.B. Wah, Power comparisons of Shapiro–Wilk, Kolmogorov–Smirnov, Lilliefors and Anderson–darling tests, J. Stat. Model. Anal. 2 (1) (2011) 21–33. https://www.nrc.gov/docs/ML1714/ML17143A100.pdf.
[44] D.S. Wilks, Statistical methods in the atmospheric sciences, in: International Geophysics Series, World Bank, Washington, DC, 2006, p. 100, https://doi.org/10.1016/S0074-6142(06)80036-7. World Bank. Global Economic Prospects, June 2020.
[45] H.E. Beck, N.E. Zimmermann, T.R. McVicar, N. Vergopolan, A. Berg, E.F. Wood, Present and future köppen-geiger climate classification maps at 1-km resolution, Sci. Data 5 (1) (2018), 180214, https://doi.org/10.1038/sdata.2018.214.
[46] I.D.E.A.M. Atlas, Climatológico de Colombia, Imprenta Nacional de Colombia, Bogotá DC, 2017. Available in: http://documentacion.ideam.gov.co/openbiblio/bvirtual/023777/023777.html.
[47] P. Sarricolea, M.J. Herrera-Ossandon, O. Meseguer-Ruiz, Climatic regionalization of continental Chile, J. Maps 13 (2) (2017) 66–73, https://doi.org/10.1080/17445647.2016.1259592.
[48] M. Mieres Brevis, La dinámica de la desigualdad en Chile: Una mirada regional, Revista de análisis económico 35 (2) (2020) 91–133, https://doi.org/10.4067/S0718-88702020000200091.
[49] M. Wang, A. Jiang, L. Gong, L. Luo, W. Guo, C. Li, J. Zheng, Ch Li, B. Yang, J. Zeng, Y. Chen, K. Zheng, H. Li, Temperature significant change COVID-19 transmission in 429 cities, medRxiv, https://doi.org/10.1101/2020.02.22.20025791, 2020.
[50] Ali Keshavarzi, Coronavirus infectious disease (COVID-19) modeling: evidence of geographical Signals, 2020. Available at SSRN: https://ssrn.com/abstract=3568425 https://doi.org/10.2139/ssrn.3568425.
[51] M. Araújo, B. Naimi, Spread of SARS-CoV-2 Coronavirus likely to be constrained by climate. https://doi.org/10.1101/2020.03.12.20034728, 2020.
[52] Bukhari Q, Jameel Y. Will coronavirus pandemic diminish by summer? SSRN: https://ssrn.com/abstract=3556998. https://doi.org/10.2139/ssrn.3556998.
[53] Y. Ma, Y. Zhao, J. Liu, X. He, B. Wang, S. Fu, et al., Effects of temperature variation and humidity on the death of COVID-19 in Wuhan, China, Sci. Total Environ. 724 (2020), 138226, https://doi.org/10.1016/j.scitotenv.2020.138226.
[54] F. Méndez-Arriaga, The temperature and regional climate effects on communitarian COVID-19 contagion in Mexico throughout phase 1, Sci. Total Environ. 735 (2020), 139560, https://doi.org/10.1016/j.scitotenv.2020.139560.
[55] A.C. Auler, F.A.M. Cássaro, V.O. da Silva, L.F. Pires, Evidence that high temperatures and intermediate relative humidity might favor the spread of COVID-19 in tropical climate: a case study for the most affected Brazilian cities, Sci. Total Environ. 729 (2020), 139090, https://doi.org/10.1016/j.scitotenv.2020.139090.
[56] R. Tosepu, J. Gunawan, D.S. Effendy, O. Ahmad, H. Lestari, H. Bahar, P. Asfian, Correlation between weather and covid-19 pandemic in Jakarta, Indonesia, Sci. Total Environ. 725 (2020), 138436, https://doi.org/10.1016/j.scitotenv.2020.138436.
[57] S. Vandini, L. Corvaglia, R. Alessandroni, G. Aquilano, C. Marsico, M. Spinelli, Respiratory syncytial virus infection in infants and correlation with meteorological factors and air pollutants, Ital. J. Pediatr. 39 (1) (2013) 1, https://doi.org/10.1186/1824-7288-39-1.
[58] J. Tan, L. Mu, J. Huang, S. Yu, B. Chen, J. Yin, An initial investigation of the association between the SARS outbreak and weather: with the view of the environmental temperature and its variation, J. Epidemiol. Community Health 59 (3) (2005) 186–192, https://doi.org/10.1136/jech.2004.020180.
[59] C. Arias-Reyes, N. Zubieta-DeUrioste, L. Poma-Machicao, F. Aliaga-Raduan, F. Carvajal-Rodriguez, M. Dutschmann, et al., Does the pathogenesis of SARS-CoV-2 virus decrease at high-altitude? Respir. Physiol. Neurobiol. 277 (2020), 103443 https://doi.org/10.1016/j.resp.2020.103443.
[60] J. Segovia-Juarez, J.M. Castagnetto, G.F. Gonzales, High altitude reduces infection rate of COVID-19 but not case-fatality rate, Respir. Physiol. Neurobiol. 281 (2020), 103494, https://doi.org/10.1016/j.resp.2020.103494.
[61] M. Pun, R. Turner, G. Strapazzon, H. Brugger, E.R. Swenson, Lower incidence of COVID-19 at high altitude: facts and confounders, High Alt. Med. Biol. 21 (3) (2020) 217–222, https://doi.org/10.1089/ham.2020.0114.
[62] M.J. Miller, J.R. Loaiza, A. Takyar, R.H. Gilman, COVID-19 in Latin America: novel transmission dynamics for a global pandemic? PLoS Neglected Trop. Dis. 14 (5) (2020), e0008265 https://doi.org/10.1371/journal.pntd.0008265.
[63] S. Kodera, E.A. Rashed, A. Hirata, Correlation between COVID-19 morbidity and mortality rates in Japan and local population density, temperature, and absolute humidity, Int. J. Environ. Res. Publ. Health 17 (15) (2020) 5477, https://doi.org/10.3390/ijerph17155477.
[64] M.S.T. Leung, S.G. Lin, J. Chow, A. Harky, COVID-19 and Oncology: Service transformation during pandemic, Cancer Med. 9 (2020) 7161–7171, https://doi.org/10.1002/cam4.3384.
[65] A. Bhadra, A. Mukherjee, K. Sarkar, Impact of population density on Covid-19 infected and mortality rate in India, Model. Earth Syst. Environ. 7 (1) (2021) 623–629, https://doi.org/10.1007/s40808-020-00984-7.
[66] K.T.L. Sy, L.F. White, B.E. Nichols, Population density and basic reproductive number of COVID-19 across United States counties, PLoS One 16 (4) (2021), e0249271, https://doi.org/10.1371/journal.pone.0249271.